Electronic Supplementary information: Quantitative photoacoustic spectral transformations in theranostic Solid Lipid Nanoparticles labelled with increasing concentrations of a Photoacoustic NIR BODIPY

Clément Linger,[a,b] Giulia Maccini,[a] Gilles Clavier,[c] Rachel Méallet,[d] Nicolas Tsapis,‡*[a] and Jérôme Gateau ‡*[b]

[a] *Institut Galien Paris-Saclay (IGPS), Université Paris-Saclay, CNRS, 91400 Orsay, France.*
[b] *Laboratoire d'Imagerie Biomédicale (LIB), Sorbonne Université, CNRS, INSERM, 75006 Paris, France.*
[c] *Photophysique et Photochimie Supramoléculaires et Macromoléculaires (PPSM), ENS Paris-Saclay, Université Paris-Saclay, CNRS, 91190, Gif-sur-Yvette, France.*
[d] *Institut des Sciences Moléculaires d'Orsay (ISMO), Université Paris-Saclay, CNRS, 91405, Orsay, France*

Table of Content

1. Material and methods

1.1. Synthesis of BODIPY-aniline palmitate.

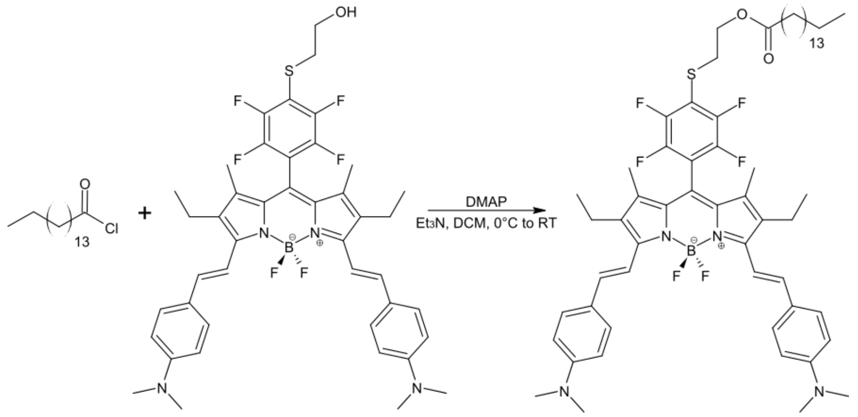

Fig. S1: Reaction scheme (esterification) to form BODIPY-aniline-palmitate (BY-aniline-Palm)

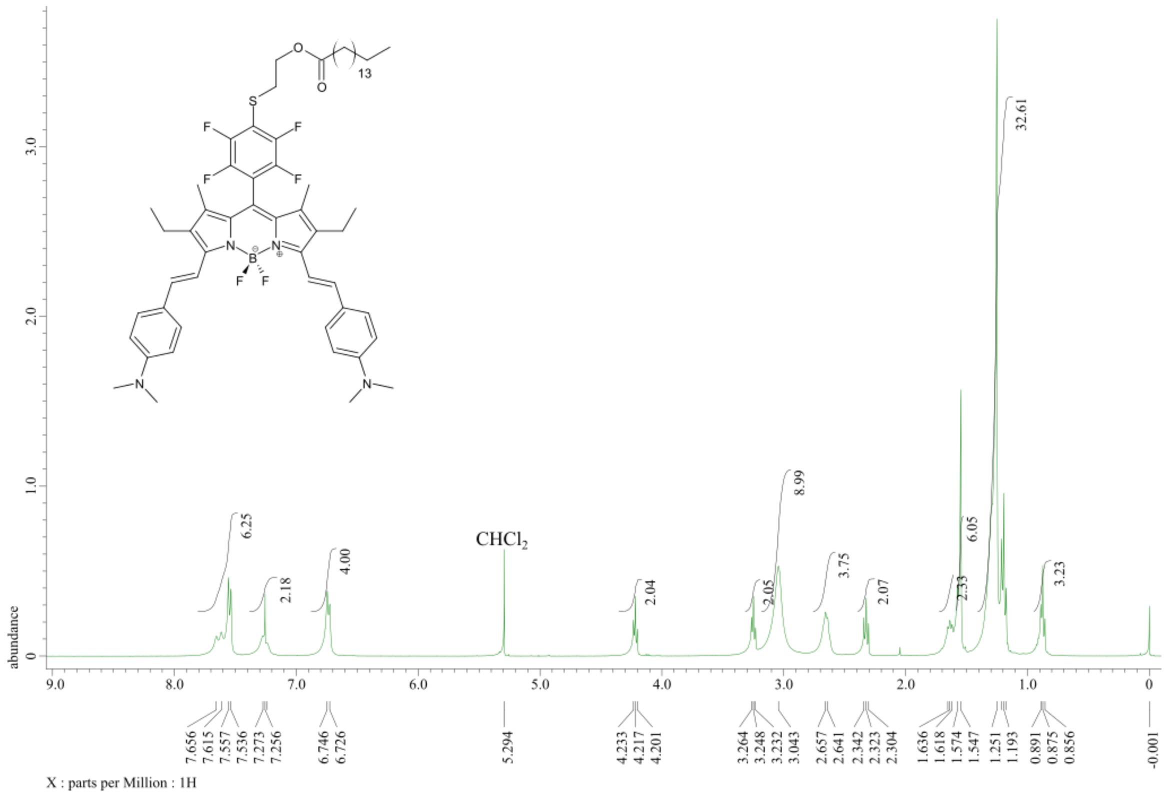

Fig. S2: [1]H NMR of BY-aniline-Palm

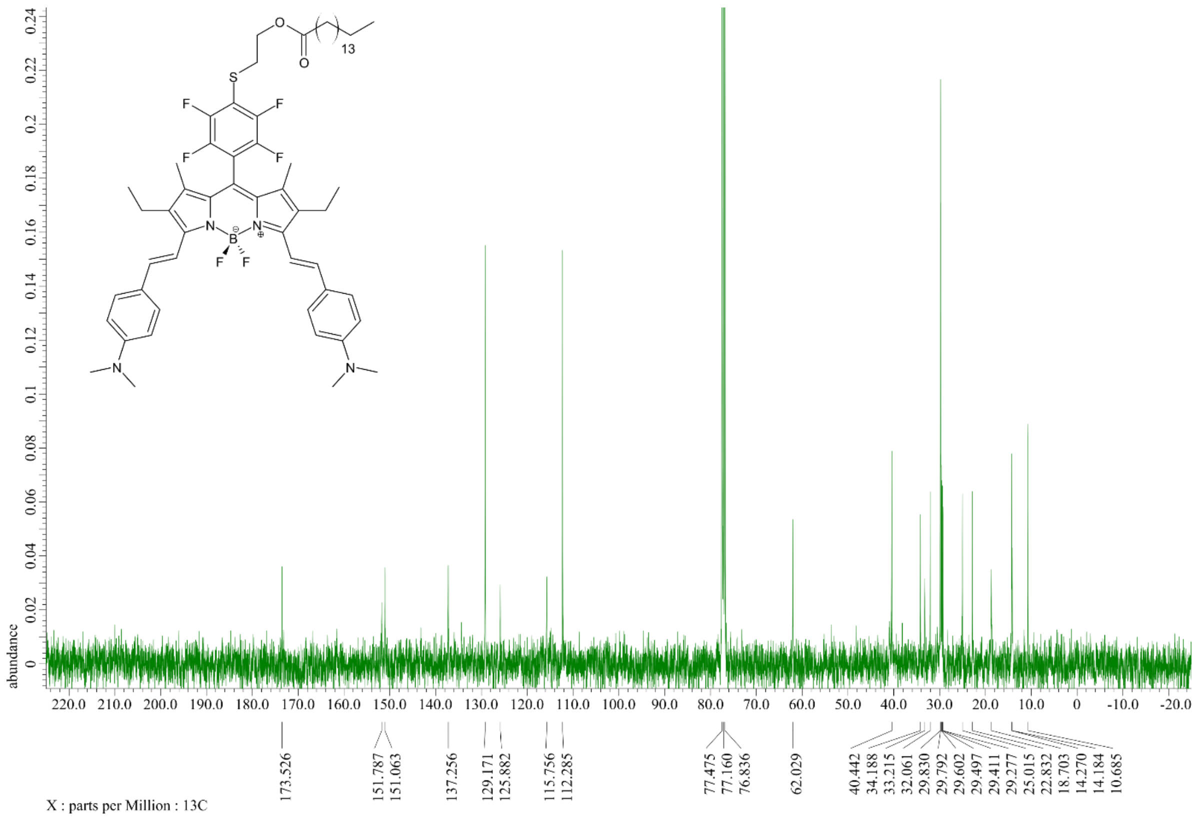

Fig. S3: ^{13}C NMR of BY-aniline-Palm

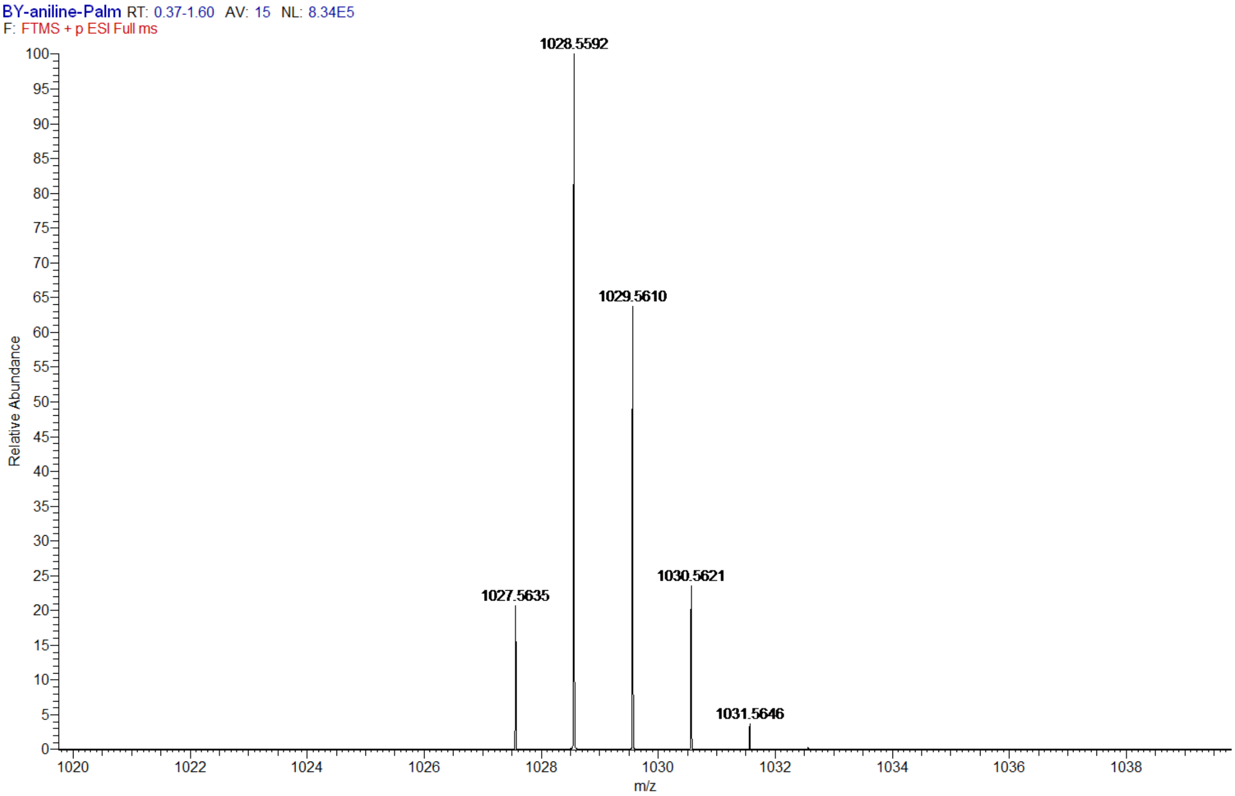

Fig. S4: HRMS (ESI) spectrum of BY-aniline-Palm

1.2. Nanoparticle Formulation

Table S1 – BY-aniline-Palm (or BY-aniline-PLA) concentrations in SLNs and PLA NPs with dilution factor to reach the same concentration.

	SLN-1%	SLN-2%	SLN-6%	SLN-12%	SLN-25%	SLN-50%	SLN-75%	SLN-100%	BY-aniline-PLA-47%
BY-aniline-Palm (or BY-aniline -PLA) concentration (mg.mL^{-1})	0.0810	0.161	0.472	0.910	1.76	3.10	4.15	5.00	2.35
BY-aniline concentration (mM)	$7.87.10^{-2}$	$1.57.10^{-1}$	$4.58.10^{-1}$	$8.84.10^{-1}$	1.71	3.01	4.04	4.86	$1.57.10^{-1}$
Dilution factor (to 1.73.10^{-2} mM)	4.5	9.0	26	51	100	169	230	280	9.0

1.3. Photophysical Measurements

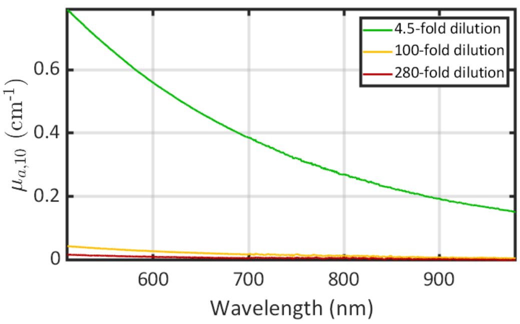

Fig. S5: Unloaded particles (SLN-0%) attenuation spectra used as blank for SLNs. The spectrum was measured for each needed dilution factor. Here 3 representative dilutions corresponding to SLN-1%, SLN-25% and SLN-100%, respectively.

1.4. Cryogenic Electron Microscopy (Cryo-EM).

Cryogenic (Transmission) Electron Microscopy was performed at Laboratoire de Physique des Solides – SOBIO Team (CNRS, Orsay, France). Drops of the solutions were deposited on copper grids covered with a holey carbon film (Quantifoil R7/2) previously treated with a plasma glow discharge (5 mA, 30 s). The excess liquid on the grids was blotted out with filter paper, and the grids were quickly immersed in liquid ethane to form a thin vitreous ice film. The whole process was performed using a Vitrobot apparatus (FEI Company). Observations were conducted at low temperature (-180 °C) on a JEOL 2010 FEG microscope (Japan) operated at 200 kV. Images were acquired with a Gatan K2 direct detection camera (USA). Typically, a stack of 20 dose-fractionated images (0.2 s acquisition/frame with a maximum dose of 20 e-/pixel/second) were recorded and then aligned to compensate for specimen motion, drift and irradiation damage with the Gatan Microscopy Suite DigitalMicrograph.

1.5. Photoacoustic Spectra Measurements

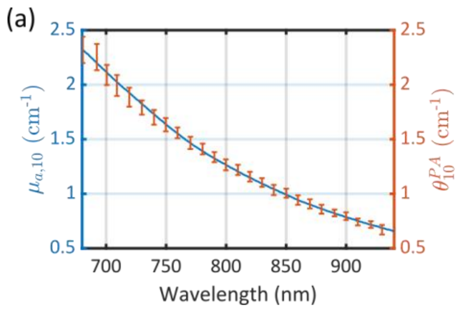

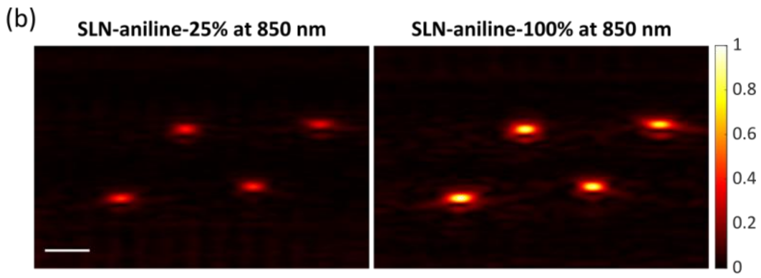

Fig. S6: (a) Absorption and PA spectra of the solution of nigrosin with a PGE equal to 1. (b) PA images of the 4 tubes obtained with the PA spectrometer for an excitation at 850 nm. These images are used to obtain the photoacoustic coefficient after calibration of the instrument. The tubes were successively filled with SLN-aniline-25% (left image) and SLN-aniline-100% (right image). The image amplitude was normalised regarding the second image because SLN-aniline-100% has a larger absorption (and PA signal) at 850 nm. The scale bar corresponds to 2 mm and the two images have the same dimensions.

2. Results

2.1. ζ Potential

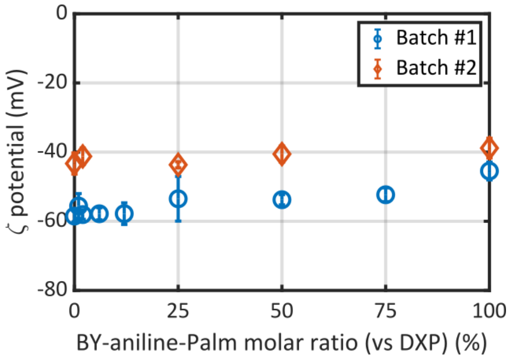

Fig. S7: Evolution of the Zeta potential as a function of the BY-aniline-Palm molar ratio (vs DXP). Markers are blue circle for Batch #1 and orange diamonds for Batch #2. Measurements were done with 20-fold dilution in NaCl 1 mM and error bars are standard deviations on 3 measurements.

2.2. Transmission Electron Microscopy and Cryo-Electron Microscopy

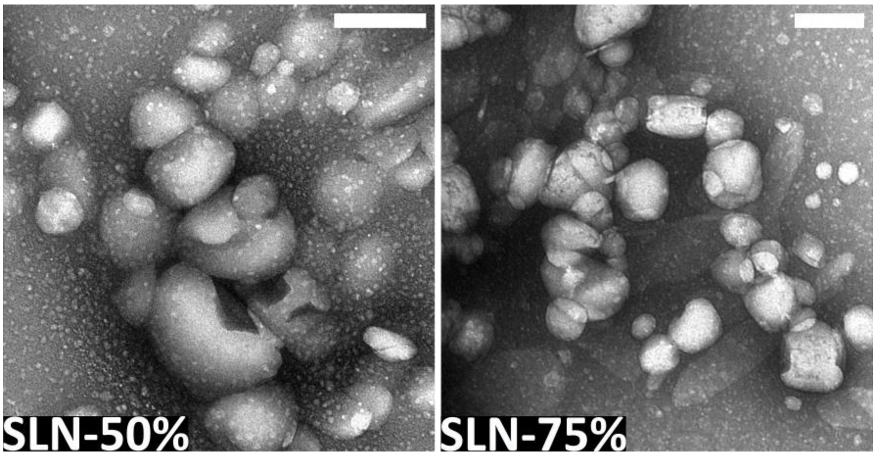

Fig. S8: TEM images of SLN-50% and SLN-75%, obtained with negative staining (uranyl acetate 2% w/w) and acquired with a JEOL JEM-1400 microscope at an acceleration voltage of 120 kV. Magnifications for SLN-50% and SLN-75% are 15,000 and 20,000, respectively. White scale bars on the top right corner represent 200 nm.

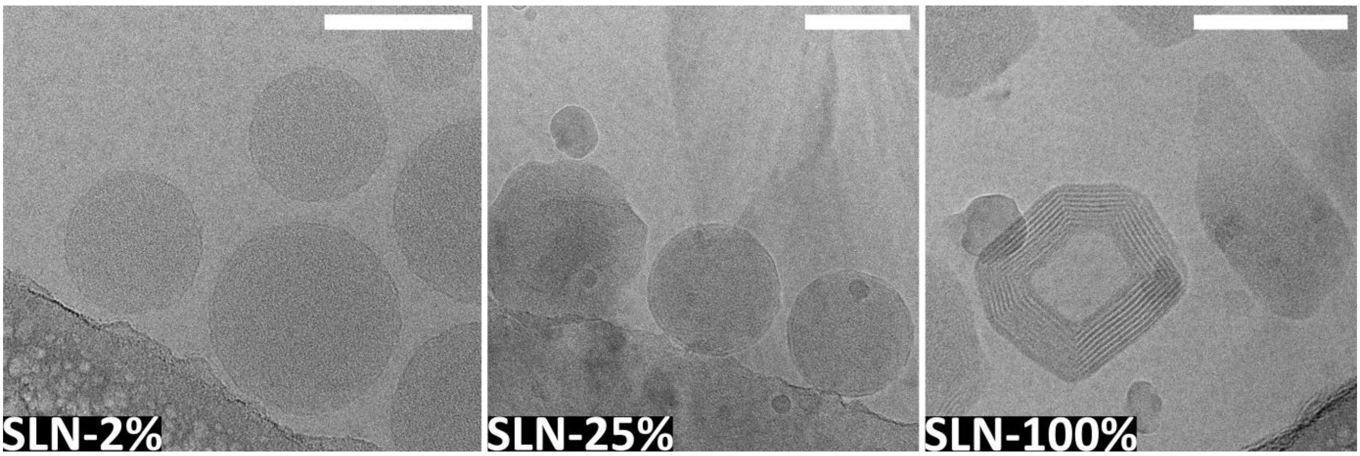

Fig. S9: Cryo-EM images of SLN-2%, SLN-25% and SLN-100% and acquired with a JEOL 2010 FEG microscope at an acceleration voltage of 200 kV. Magnifications for SLN-2%; SLN-SLN-25% and SLN-100% are 30,000; 28,000 and 52,000, respectively. White scale bars on the top right corner represent 100 nm.

2.3. Absorption coefficient per mole of particles

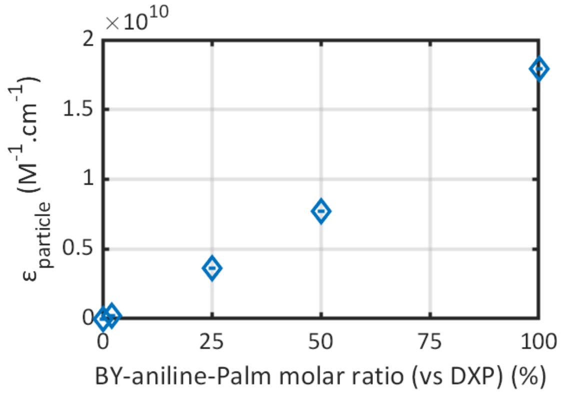

Fig. S10: Evolution of the absorption cross section per mole of particles evaluated at the maximum absorption wavelength ($\varepsilon_{\text{particle}}$) as a function of the BY-aniline-Palm molar ratio (vs DXP) and determined on Batch #2.

2.4. Absorption spectra of BY-aniline-Palm and BY-aniline-PLA

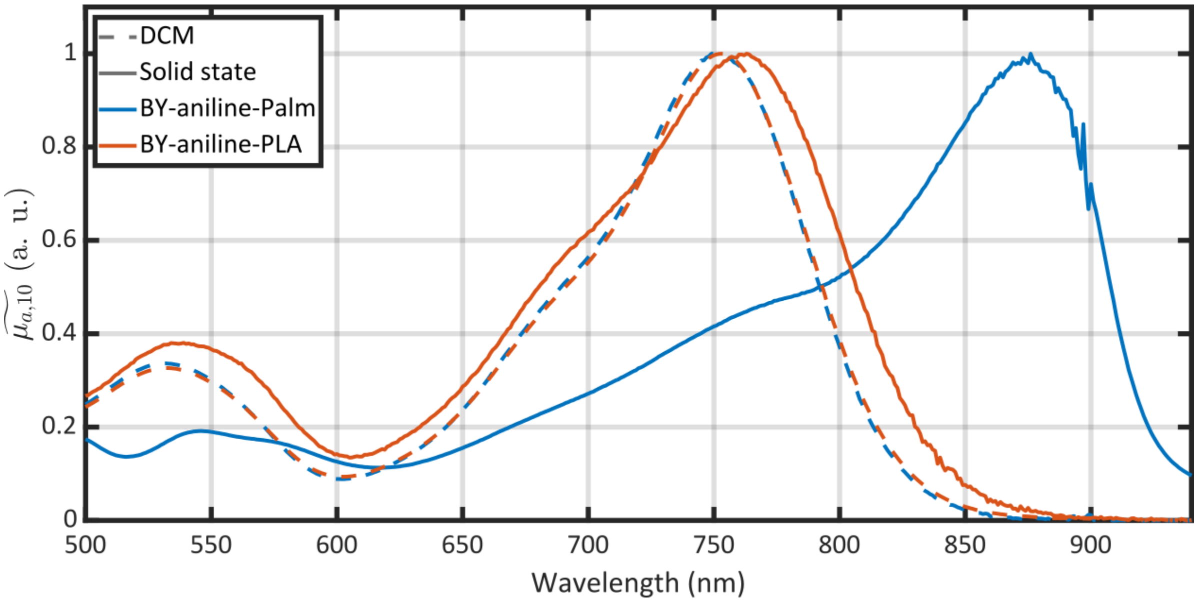

Fig. S11: BY-aniline-Palm and BY-aniline-PLA absorption spectra in solution (DCM) and solid-state. Spectra are normalized for the sake of readability ($\widetilde{\mu_{a,10}}$).

2.5. Fluorescence, absorption and photoacoustic spectra of nanoparticles

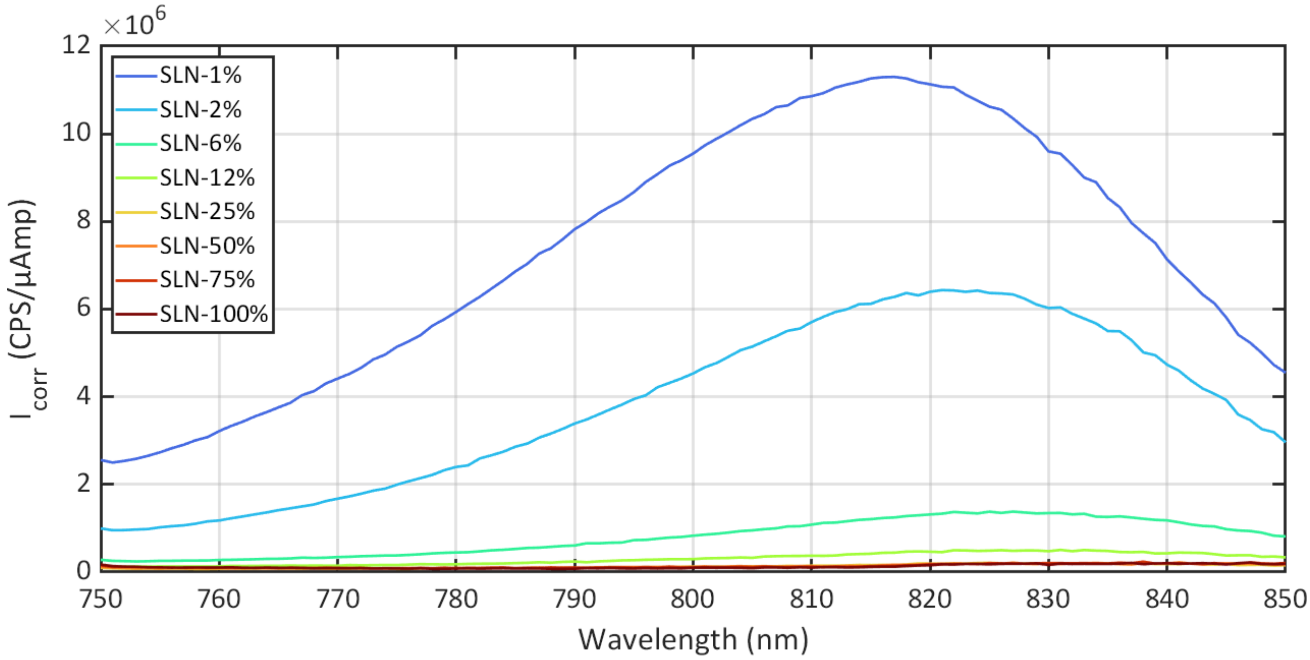

Fig. S12: Fluorescence spectrum (λ_{ex} = 730 nm, slits width 10 nm and A < 0.1) of each type of SLN. The amplitude was corrected by the absorbance at 730 nm.

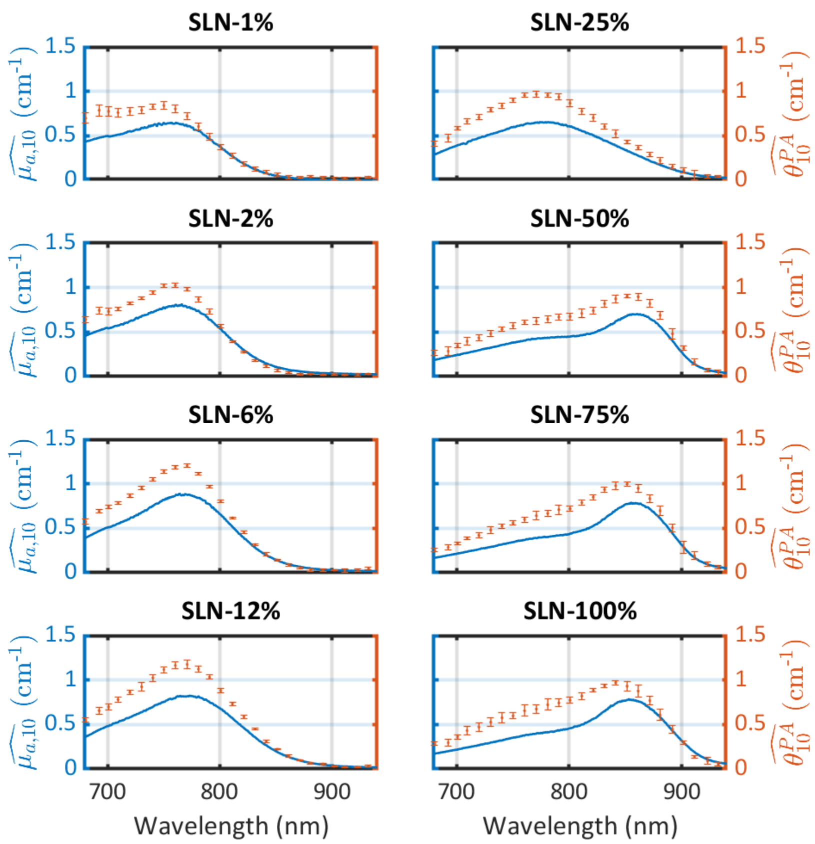

Fig. S13: Superposition of the absorption (blue) and PA (orange) spectra for each SLN (Batch #1).

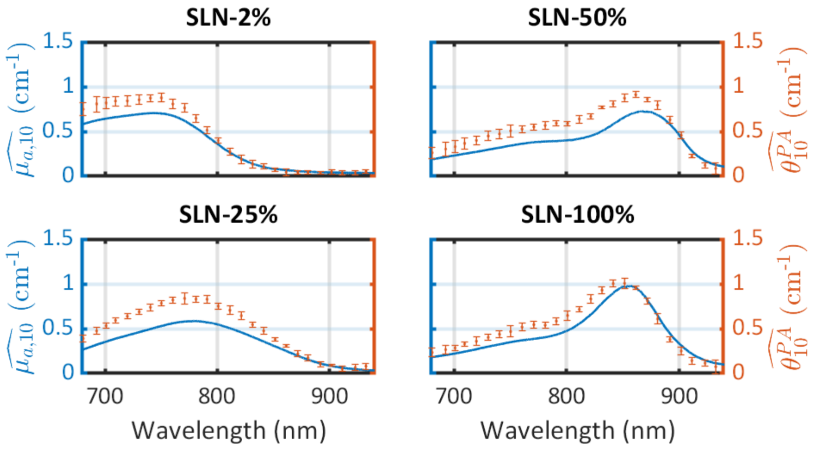

Fig. S14: Superposition of the absorption (blue) and PA (orange) spectra for each SLN (Batch #2).

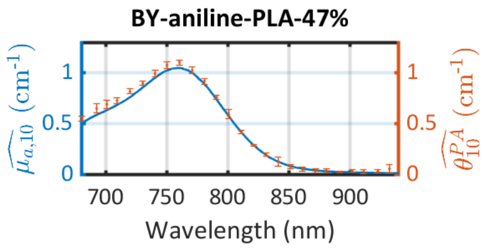

Fig. S15: Superimposition of the absorption (blue) and PA (orange) spectra for BY-aniline-PLA-47% NPs.

2.6. Spectra modelling

Table S2 – Parameters determined for the Gaussian decomposition of the absorption spectra and the PA spectra of Batch #1. a_i (cm^{-1}) is the amplitude of the gaussian curve, λ_i (nm) is the central wavelength and ω_i (nm) is proportional to the full width half maximum ($FWHM_i = 2\sqrt{2\ln 2}\cdot\omega_i$). Band photoacoustic efficiencies (BPAE) were defined as in the Material and Methods section as the ratio between the PA band area and the corresponding absorption band area. As the widths ω_i are set equal for PA and absorption, BPAE corresponds to an amplitude ratio.

			SLN-1%	SLN-2%	SLN-6%	SLN-12%	SLN-25%	SLN-50%	SLN-75%	SLN-100%
Absorp-tion	**Gaussian #1**	a_1						0.51	0.56	0.53
		λ_1						865	864	863
		ω_1						26.5	26.5	26.5
	Gaussian #2	a_2	0.57	0.73	0.85	0.80	0.63	0.42	0.40	0.43
		λ_2	765	769	770	773	783	789	798	799
		ω_2	37.4	39.8	41.8	46.5	59.5	58.6	59.5	59.5
	Gaussian #3	a_3	0.4	0.4	0.31	0.26	0.15	0.11	0.11	0.12
		λ_3	685	685	685	685	685	685	685	685
		ω_3	41.0	41.6	38.0	38.0	45.2	49.4	52.8	46.2
PA	**Gaussian #1**	a'_1						0.60	0.59	0.51
		λ'_1						863	860	858
		ω_1						26.5	26.5	26.5
	Gaussian #2	a'_2	0.66	0.89	1.13	1.12	0.94	0.65	0.67	0.72
		λ'_2	762	764	767	769	778	791	799	797
		ω_2	37.4	39.8	41.8	46.5	59.5	58.6	59.5	59.5
	Gaussian #3	a'_3	0.64	0.53	0.44	0.35	0.18	0.16	0.17	0.18
		λ'_3	685	685	685	685	685	685	685	685
		ω_3	41.0	41.6	38.0	38.0	45.2	49.4	52.8	46.2
BPAE	**Gaussian #1**	$\frac{a'_1}{a_1}$						1.18	1.06	0.96
	Gaussian #2	$\frac{a'_2}{a_2}$	1.16	1.21	1.33	1.41	1.49	1.54	1.67	1.70
	Gaussian #3	$\frac{a'_3}{a_3}$	1.61	1.32	1.41	1.37	1.19	1.41	1.52	1.55

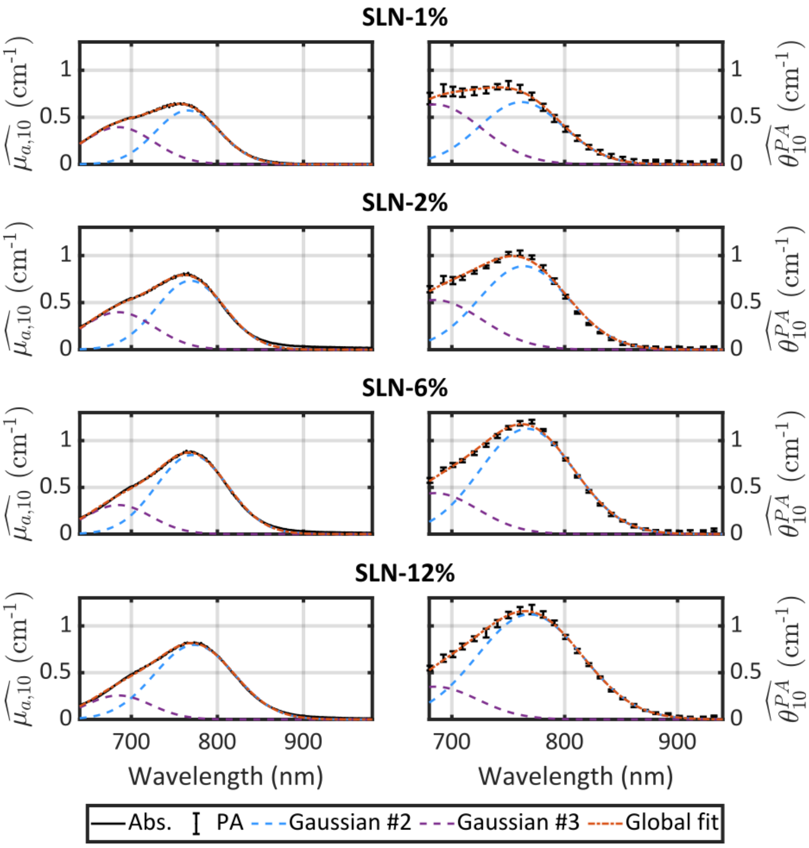

Fig. S16: Gaussian decomposition of absorption and PA spectra for SLN of Batch #1 with BY-aniline-Palm percentage below 25% (excluded).

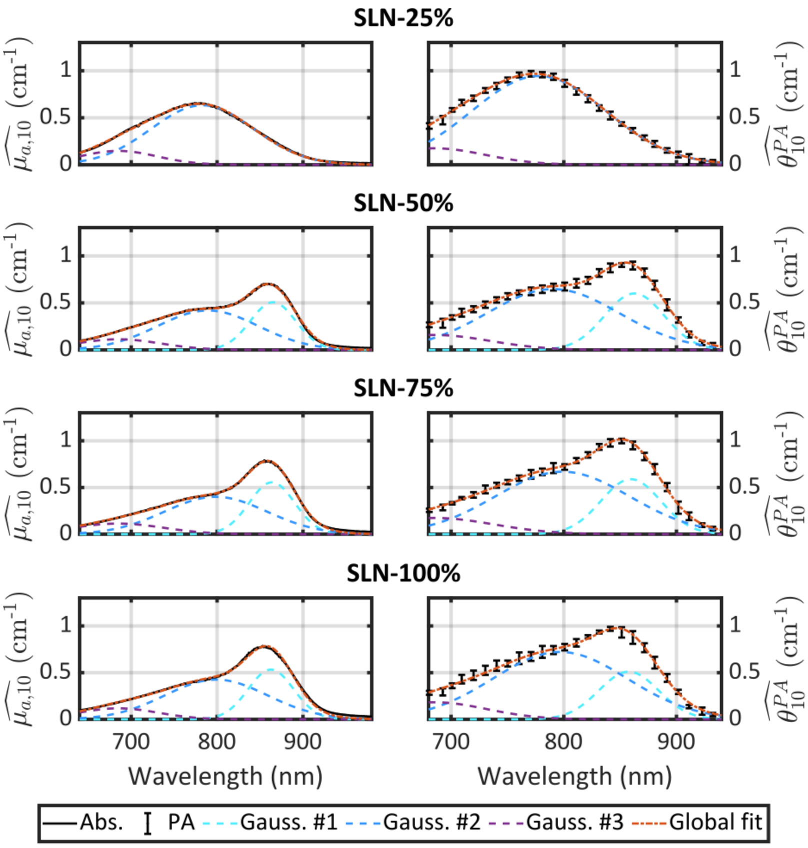

Fig. S17: Gaussian decomposition of absorption and PA spectra for SLN of Batch #1 with BY-aniline-Palm percentage above 25% (included)

Table S3 – Parameters determined for the Gaussian decomposition of the absorption spectra and the PA spectra of Batch #2 and BY-anilne-PLA-47%. a_i (cm^{-1}) is the amplitude of the gaussian curve, λ_i (nm) is the central wavelength and ω_i (nm) is proportional to the full width half maximum ($FWHM_i = 2\sqrt{2\ln 2} \cdot \omega_i$). BPAE was defined as in Table S2.

			SLN-2%	**SLN-25%**	**SLN-50%**	**SLN-100%**	**BY-aniline-PLA-47%**
Absorption	**Gaussian #1**	a_1			0.56	0.71	
		λ_1			875	859	
		ω_1			26.5	26.5	
	Gaussian #2	a_2	0.47	0.56	0.40	0.41	0.96
		λ_2	763	784	799	799	764
		ω_2	43.2	59.5	59.5	59.5	37.3
	Gaussian #3	a_3	0.50	0.14	0.14	0.13	0.43
		λ_3	685	685	685	685	685
		ω_3	54.0	45.3	46.5	46.2	40.3
PA	**Gaussian #1**	a'_1			0.61	0.66	
		λ'_1			870	854	
		ω_1			26.5	26.5	
	Gaussian #2	a'_2	0.56	0.81	0.59	0.55	1.00
		λ'_2	759	779	800	797	764
		ω_2	43.2	59.5	59.5	59.5	37.3
	Gaussian #3	a'_3	0.63	0.20	0.21	0.15	0.47
		λ'_3	685	685	685	685	685
		ω_3	54.0	45.3	46.5	46.2	40.3
BPAE	**Gaussian #1**	$\frac{a'_1}{a_1}$			1.09	0.93	
	Gaussian #2	$\frac{a'_2}{a_2}$	1.19	1.44	1.46	1.32	1.04
	Gaussian #3	$\frac{a'_3}{a_3}$	1.26	1.38	1.45	1.16	1.11

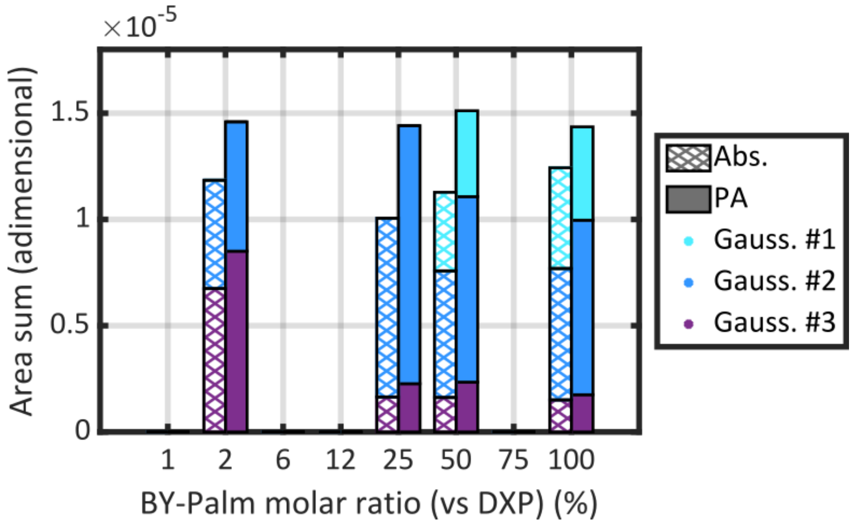

Fig. S18: Contribution of each Gaussian function (area) in the total spectrum area for each SLN of Batch #2. Absorption spectra are on the left-hand side in hatched bars while PA spectra are on the right-hand side in coloured bars.

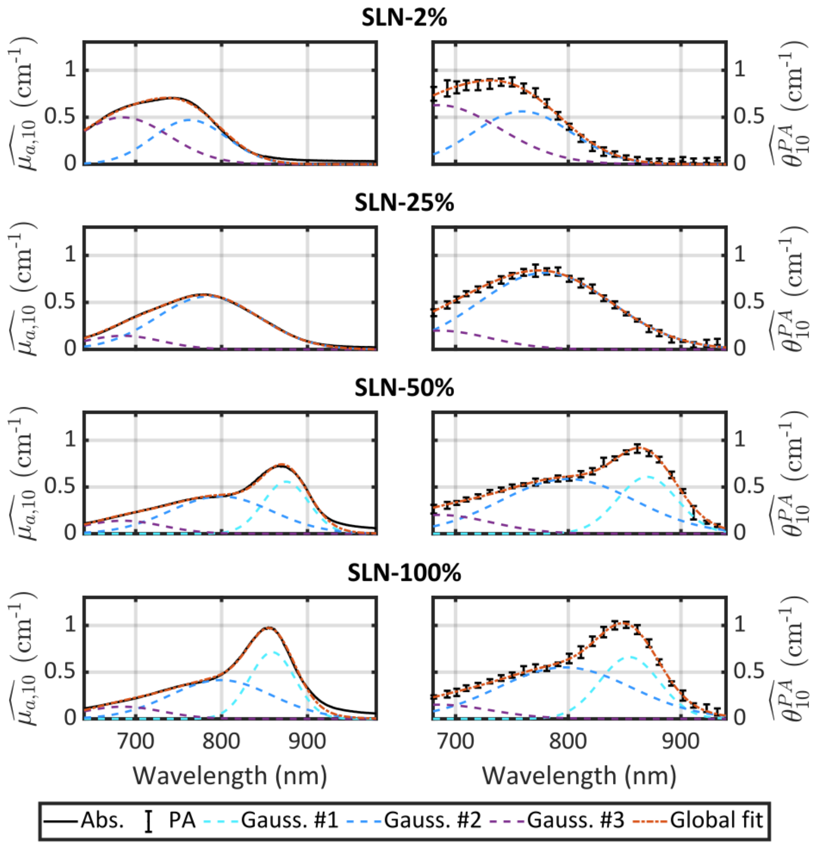

Fig. S19: Gaussian decomposition of absorption and PA spectra for SLNs of Batch #2.

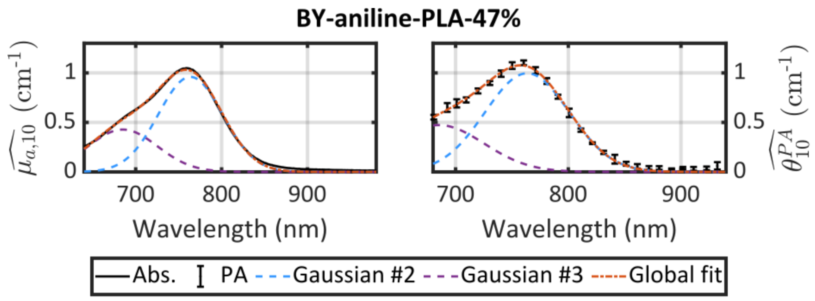

Fig. S20: Gaussian decomposition of absorption and PA spectra for BY-aniline-PLA-47%

2.7. Photoacoustic spectra at different temperatures

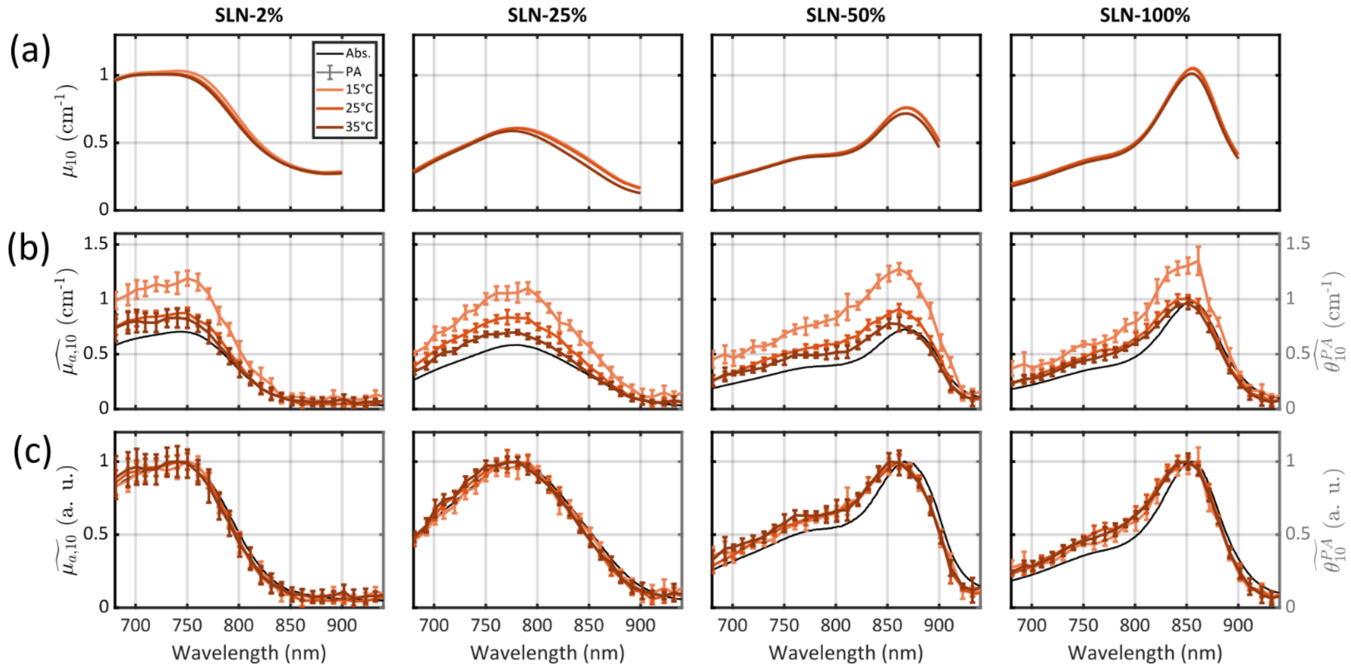

Fig. S21: (a) Absorbance spectra measured at three temperatures (15°C, 25°C and 35°C) of SLNs from batch #2. Measurements at different temperatures are color-coded with shades of orange. The scattering was not corrected. (b) PA spectra at three temperatures (15°C, 25°C and 35°C) of SLNs. The absorption spectra (corrected for scattering) are displayed with a black solid line. (c) Normalized absorption and PA spectra at three temperatures (15°C, 25°C and 35°C) of SLNs. Each spectrum is normalized by the spectrum maximum. The colour code is the same in (a), (b) and (c).

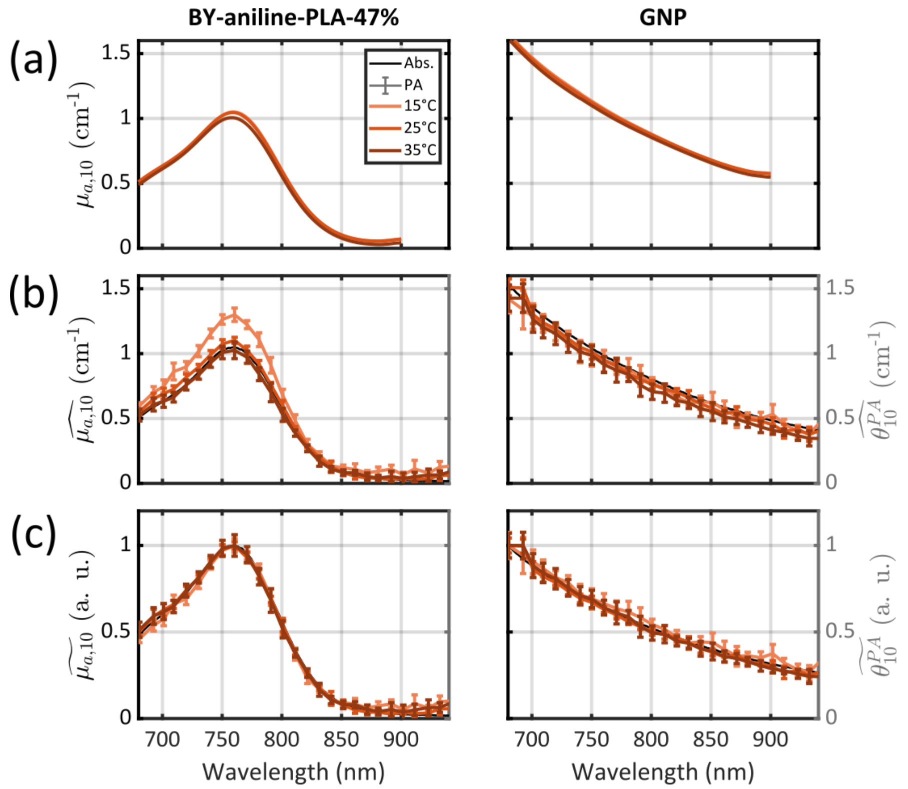

Fig. S22: (a) Absorbance spectra measured at three temperatures (15°C, 25°C and 35°C) of PLA NPs (left) and GNPs (right). Measurements at different temperatures are color-coded with shades of orange. The scattering was not corrected. (b) PA spectra at three temperatures (15°C, 25°C and 35°C) of PLA NPs (left) and GNPs (right). The absorption spectra (corrected for scattering) are displayed with a black solid line. (c) Normalized absorption and PA spectra at three temperatures (15°C, 25°C and 35°C) of PLA NPs (left) and GNPs (right). Each spectrum is normalized by the spectrum maximum. The colour code is the same in (a) (b) and (c).

Table S4 – Global photoacoustic efficiencies (GPAE) for Batch #1 were defined in the Material and Method section as the ratio between the integral of the PA spectrum and the integral of the equivalent absorption spectrum on the interval [680 nm, 920 nm]. It corresponds as the weighted mean PGE over the whole spectrum.

	SLN-1%	SLN-2%	SLN-6%	SLN-12%	SLN-25%	SLN-50%	SLN-75%	SLN-100%
GPAE 25°C	1.31	1.21	1.32	1.39	1.43	1.4	1.44	1.43

Table S5 – Global photoacoustic efficiencies (GPAE) for Batch #2, GNP and BY-aniline-PLA-47% were computed as defined in Table S4.

	SLN-2%	SLN-25%	SLN-50%	SLN-100%	BY-aniline-PLA-47%	GNP
GPAE 15°C	1.65	1.84	1.88	1.47	1.24	0.96
GPAE 25°C	1.2	1.4	1.34	1.15	1.05	0.97
GPAE 35°C	1.16	1.19	1.17	1.08	0.98	0.92

2.8. Photostability under laser excitation

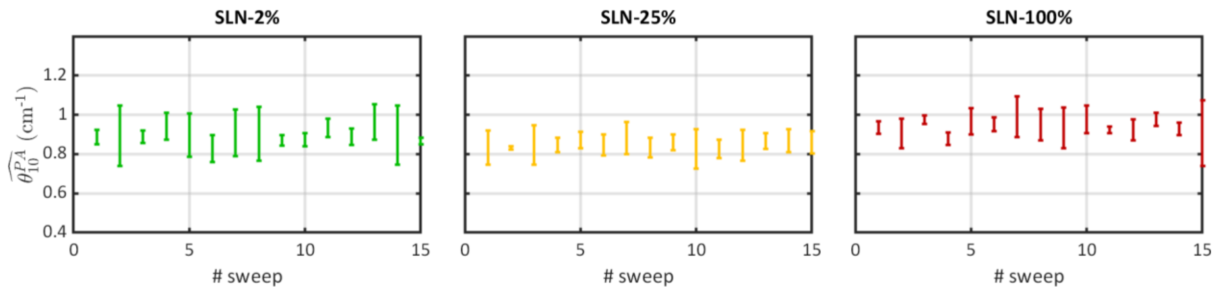

Fig. S23: Photoacoustic coefficients as a function of the number of the sweeps. The PA coefficients are measured at the maximum absorption wavelength, namely : 750 nm for SLN-2% (green), 780 nm for SLN-25% (yellow) and 960 nm for SLN-100% (red), respectively. For each sweep, the acquisition was performed simultaneously on four tubes and the displayed results corresponds to the median (with the MAD as error bar) over the 4 tubes.

2.9. Photoacoustic signal variability with the laser fluence

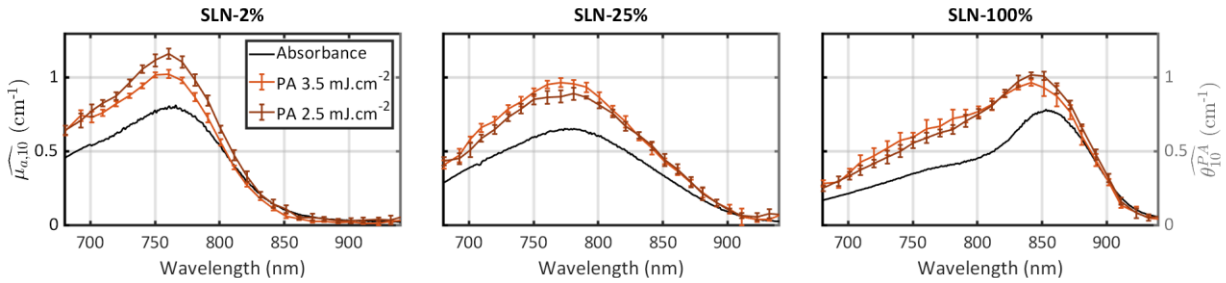

Fig. S24: Superimposition of the absorption and PA spectra for three formulations (SLN-2%, SLN-25% and SLN-100%). Two different laser fluences are used: 3.5 mJ.cm^{-2} (orange) and 2.5 mJ.cm^{-2} (brown). The mean variation between the spectra at the two fluences is below 10%.

2.10. Transient absorption signal

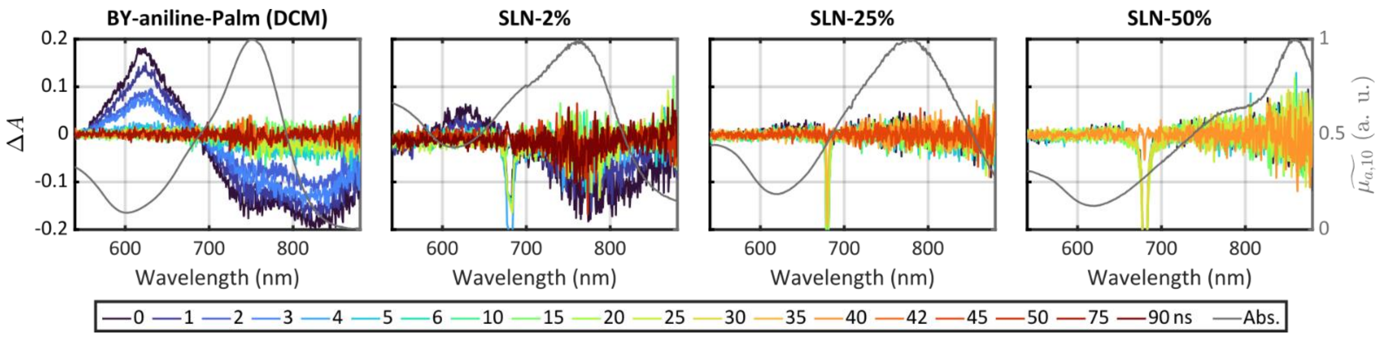

Fig. S25: Transient absorption spectra of BY-aniline-Palm in DCM, SLN-2%, SLN-25% and SLN-50% for different time delays (in ns and color-coded) between pump (at 680 nm) and probe. Normalized equivalent absorption spectra are displayed in grey.